

## Biofuel Cells

How to cite: *Angew. Chem. Int. Ed.* **2020**, *59*, 16506–16510

International Edition: doi.org/10.1002/anie.202006824

German Edition: doi.org/10.1002/ange.202006824

**Redox-Polymer-Based High-Current-Density Gas-Diffusion H<sub>2</sub>-Oxidation Bioanode Using [FeFe] Hydrogenase from *Desulfovibrio desulfuricans* in a Membrane-free Biofuel Cell**

Julian Szczesny, James A. Birrell, Felipe Conzuelo, Wolfgang Lubitz,\* Adrian Ruff,\* and Wolfgang Schuhmann\*

**Abstract:** The incorporation of highly active but also highly sensitive catalysts (e.g. the [FeFe] hydrogenase from *Desulfovibrio desulfuricans*) in biofuel cells is still one of the major challenges in sustainable energy conversion. We report the fabrication of a dual-gas diffusion electrode H<sub>2</sub>/O<sub>2</sub> biofuel cell equipped with a [FeFe] hydrogenase/redox polymer-based high-current-density H<sub>2</sub>-oxidation bioanode. The bioanodes show benchmark current densities of around 14 mA cm<sup>-2</sup> and the corresponding fuel cell tests exhibit a benchmark for a hydrogenase/redox polymer-based biofuel cell with outstanding power densities of 5.4 mW cm<sup>-2</sup> at 0.7 V cell voltage. Furthermore, the highly sensitive [FeFe] hydrogenase is protected against oxygen damage by the redox polymer and can function under 5 % O<sub>2</sub>.

In the transition from fossil fuels to a sustainable energy economy, a sustainable solution to store excess electrical energy is to generate H<sub>2</sub> by water electrolysis.<sup>[1–4]</sup> H<sub>2</sub> can then be oxidized as a fuel on demand at an electrode modified with an appropriate electrocatalyst, while O<sub>2</sub> is reduced to water at a suitable cathode.<sup>[3]</sup> The most commonly applied electrocatalysts in H<sub>2</sub>/O<sub>2</sub> fuel cells are based on scarce and costly noble metals like Pt and Ir.<sup>[1]</sup> Evidently, for a sustainable and economic process, electrocatalysts based on abundant materials are highly desired.

Nature has evolved highly efficient biocatalysts, hydrogenases, for the reversible conversion of H<sub>2</sub>, using active centers consisting solely of earth-abundant metals, namely Ni and Fe,<sup>[5]</sup> and with a catalytic performance similar to that of Pt.<sup>[4–7]</sup> Hydrogenases have already been employed in the anode of H<sub>2</sub>/O<sub>2</sub> biofuel cells,<sup>[7–10]</sup> typically in combination with multi-copper oxidase (bilirubin oxidase or laccase)-based O<sub>2</sub>-reducing biocathodes.<sup>[11]</sup> The high activity of hydrogenases correlates with high sensitivity towards O<sub>2</sub> as well as high-potential inactivation, which hampers their integration in potentially useful devices. Hence, such devices are restricted to the lab scale.<sup>[7–9,12,13]</sup> In particular, [FeFe] hydrogenases are among the most active biocatalysts for H<sub>2</sub>-oxidation; however, they suffer from extreme and irreversible O<sub>2</sub> deactivation, rapid inactivation at high potentials, and degradation under light irradiation.<sup>[5,7,14]</sup> While the less sensitive [NiFe] and [NiFeSe] hydrogenases have been integrated in high-performance dual-gas diffusion electrodes<sup>[15,16]</sup> as well as gas diffusion biofuel cells,<sup>[17–20]</sup> the use of [FeFe] hydrogenases in such devices has not—to the best of our knowledge—been described so far and applications are often limited to glovebox conditions.<sup>[14,21,22]</sup>

The use of low-potential viologen-modified redox polymers as immobilization, wiring, and protection matrix<sup>[23–25]</sup> ensured the use of various hydrogenases in conventional<sup>[22,23]</sup> and membrane-free dual-gas diffusion H<sub>2</sub>/O<sub>2</sub> biofuel cells.<sup>[20,26]</sup> Even the highly sensitive [FeFe] hydrogenase could be integrated in a conventional H<sub>2</sub>/O<sub>2</sub> biofuel cell in combination with an O<sub>2</sub>-reducing bilirubin oxidase biocathode.<sup>[22]</sup> However, the system was limited by mass transport and the power output was similar to fuel cells based on [NiFe]<sup>[23]</sup> and [NiFeSe]<sup>[26]</sup> hydrogenases. Thus, immobilization of the highly active [FeFe] hydrogenase into gas diffusion layers is greatly desired.<sup>[12,15,27]</sup> Stimulated by our previous findings,<sup>[20,26]</sup> we exploited the possibility to construct a redox polymer/[FeFe] hydrogenase high-current-density gas diffusion bioanode for H<sub>2</sub>-oxidation that can be introduced into a membrane-free biofuel cell. As the active H<sub>2</sub>-oxidation catalyst we selected the [FeFe] hydrogenase from *Desulfovibrio desulfuricans* (DdHydAB), which is one of the most active hydrogenases for H<sub>2</sub>-oxidation with turnover frequencies of up to 63 000 s<sup>-1</sup>.<sup>[14,21]</sup>

As the electrode material, carbon-cloth-based gas diffusion layers were used for the immobilization of polymer/hydrogenase layers and the construction of high-current-density H<sub>2</sub>-oxidation bioanodes as shown earlier for other types of hydrogenases.<sup>[20,26]</sup>

[\*] J. Szczesny, Dr. F. Conzuelo, Dr. A. Ruff, Prof. Dr. W. Schuhmann Analytical Chemistry—Center for Electrochemical Sciences (CES) Faculty of Chemistry and Biochemistry, Ruhr University Bochum Universitätsstr. 150, 44780 Bochum (Germany) E-mail: adrian.ruff@rub.de wolfgang.schuhmann@rub.de

Dr. J. A. Birrell, Prof. Dr. W. Lubitz Max Planck Institute for Chemical Energy Conversion Stiftstrasse 34–36, 45470 Mülheim an der Ruhr (Germany) E-mail: wolfgang.lubitz@cec.mpg.de

Dr. A. Ruff Present address: PPG (Deutschland) Business Support GmbH PPG Packaging Coatings Erlenbrunnenstr. 20, 72411 Bodelshausen (Germany)

Supporting information and the ORCID identification number(s) for the author(s) of this article can be found under: <https://doi.org/10.1002/anie.202006824>.

© 2020 The Authors. Published by Wiley-VCH Verlag GmbH & Co. KGaA. This is an open access article under the terms of the Creative Commons Attribution License, which permits use, distribution and reproduction in any medium, provided the original work is properly cited.

For the electrical wiring of DdHydAB, the redox polymers P(N<sub>3</sub>MA-BA-GMA)-vio (poly(3-azido-propyl methacrylate-*co*-butyl acrylate-*co*-glycidyl methacrylate)-viologen) and P(GMA-BA-PEGMA)-vio (poly(glycidyl methacrylate-*co*-butyl acrylate-*co*-poly(ethylene glycol)methacrylate)-viologen) were integrated in a double-layer configuration (Figure 1) analogous to systems based on [NiFe] and [NiFeSe] hydrogenases that were described previously.<sup>[20,25]</sup> The less hydrophilic P(GMA-BA-PEGMA)-vio (lower viologen content, < 65 mol %, compared to P(N<sub>3</sub>MA-BA-GMA)-vio, 71 mol %) is used as an adhesion layer between the active P(N<sub>3</sub>MA-BA-GMA)-vio/hydrogenase layer (green part in Figure 1) and the rather hydrophobic carbon cloth.<sup>[20]</sup> Both polymers are modified with the same viologen species with

the redox potential of  $\approx -0.3$  V vs. SHE,<sup>[20]</sup> which is approximately 0.11 V more positive than the potential of the H<sub>2</sub>/H<sup>+</sup> couple at neutral pH and at 298.15 K ( $-0.414$  V vs. SHE). This allows for a high driving force for H<sub>2</sub>-oxidation but is still low enough to ensure a high open circuit voltage (OCV) in a corresponding biofuel cell that depends on the potential gap between bioanode and biocathode.<sup>[30]</sup> We want to emphasize that redox polymers additionally act as pseudo-capacitive elements which further increase the OCV due to charging of the immobilized polymer matrix leading to a shift in open circuit potential under turnover conditions (see Note S1 in the Supporting Information and refs. [31,32]).

The carbon-cloth-based electrodes were modified in a sequential drop-cast process. First the (P(GMA-BA-PEGMA)-vio) adhesion layer was deposited and dried on the electrodes followed by immobilization of the catalytically active layer (P(N<sub>3</sub>MA-BA-GMA)-vio/DdHydAB). The double-layer electrodes will be designated as P(GMA-BA-PEGMA)-vio/P(N<sub>3</sub>MA-BA-GMA)-vio/DdHydAB in the following. The electrodes were prepared under glovebox conditions. For measurements, the electrodes were transferred under Ar atmosphere using standard Schlenk techniques and mounted into the gas diffusion electrochemical cell<sup>[20]</sup> that was installed in a conventional fumehood.

Cyclic voltammograms (Figure 2a) recorded with P(GMA-BA-PEGMA)-vio/P(N<sub>3</sub>MA-BA-GMA)-vio/DdHydAB electrodes under turnover conditions (H<sub>2</sub> gas diffusion mode, red curve) show pronounced catalytic oxidation waves with absolute steady state currents of up to 2.0 mA at +0.2 V vs. SHE, which accounts for a current density of  $\approx 16$  mA cm<sup>-2</sup> (referenced to the modified surface area on the carbon cloth substrate, diameter of polymer spot  $\approx 4$  mm). The half-wave potential of the catalytic wave ( $-0.16$  V vs. SHE) is slightly above the midpoint potential of the polymer-bound viologen species (Figure 2a, black curves,  $-0.3$  V); however, the onset potential of the H<sub>2</sub>-oxidation wave matches the redox potential of the polymer-bound viologen units confirming mediated electron transfer, which is crucial for an effective protection of the sensitive enzyme.<sup>[23]</sup> The shift of the half-wave potential to more positive values as compared to the midpoint potential of the mediator might be due to *iR* drop at these rather high current values. This is corroborated by the large peak potential separation of  $\approx 130$  mV in the voltammograms recorded under non-turnover conditions. High potential inactivation at  $> 0$  V vs. SHE is absent, showing that the polymer indeed acts as a potential shield (Nernst buffer)<sup>[23]</sup> for this sensitive protein.

Average H<sub>2</sub> steady-state oxidation currents were calculated to be  $1.8 \pm 0.3$  mA/ $14.1 \pm 2.1$  mA cm<sup>-2</sup> ( $n = 3$ ; Table S1). The values exceed current densities obtained in direct electron transfer, with the enzyme wired to graphite electrodes ( $350$ – $450$   $\mu$ A cm<sup>-2</sup>),<sup>[14,21]</sup> demonstrating the advantage of the 3D polymer matrix which ensures wiring of a large amount of enzyme independent of its orientation and location on the electrode surface as well as the enhanced mass transport ensured by the gas diffusion layer.

The operational stability of the P(GMA-BA-PEGMA)-vio/P(N<sub>3</sub>MA-BA-GMA)-vio/DdHydAB electrode was evaluated by chronoamperometry showing a current loss of

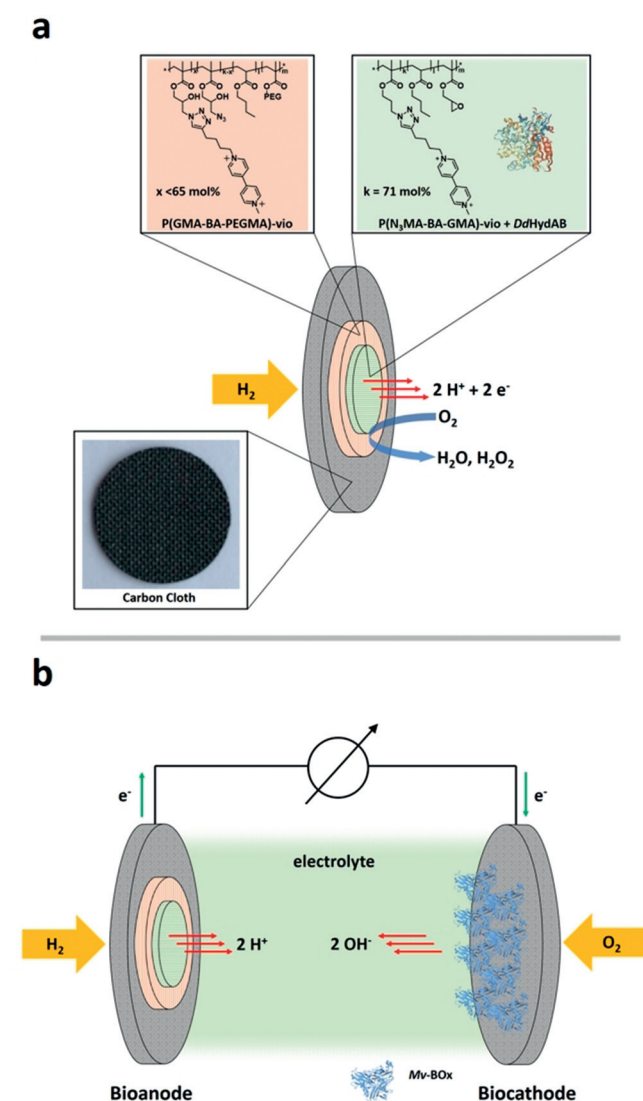


**Figure 1.** a) Scheme of the proposed multilayer gas diffusion electrode modified with the DdHydAB (1HFE<sup>[28]</sup>) hydrogenase wired through the viologen-modified polymers P(GMA-BA-PEGMA)-vio and P(N<sub>3</sub>MA-BA-GMA)-vio. b) Schematic of the dual gas diffusion membrane-free H<sub>2</sub>/O<sub>2</sub> powered biofuel cell equipped with the bioanode depicted in (a) and an O<sub>2</sub>-reducing bilirubin oxidase (6IQZ<sup>[29]</sup>) based biocathode operated in a direct electron transfer regime. Not drawn to scale.

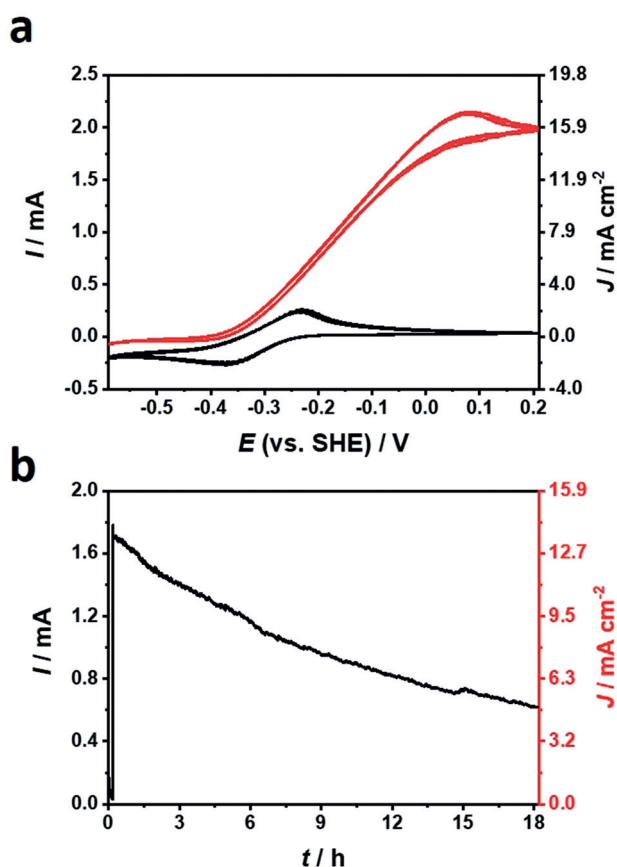


**Figure 2.** Electrochemical characterization of the redox polymer/DdHydAB-based bioanode. a) Cyclic voltammograms ( $5 \text{ mVs}^{-1}$ ) of a P(GMA-BA-PEGMA)-vio//P(N<sub>3</sub>MA-BA-GMA)-vio/DdHydAB gas-diffusion bioanode in the presence of H<sub>2</sub> (red traces, three consecutive CVs) and Ar (black traces, three consecutive CVs). B) Chronoamperometry of a P(GMA-BA-PEGMA)-vio//P(N<sub>3</sub>MA-BA-GMA)-vio/DdHydAB bioanode at an applied potential of +0.16 V vs. SHE and in H<sub>2</sub> gas diffusion mode. Working electrolyte: 0.1 M phosphate buffer (pH 7.4); nominal hydrogenase loading:  $39.8 \text{ nmol cm}^{-2}$ , total polymer loading:  $1.8 \text{ mg cm}^{-2}$ .

$\approx 50\%$  of the initial current after 11 h (Figure 2b), while after 18 h of operation the current dropped to 35% of the initial value. In comparison, a gas diffusion electrode based on a less sensitive [NiFe] hydrogenase wired with the same redox polymer double-layer architecture shows a 50% drop after  $\approx 13 \text{ h}$ .<sup>[20]</sup> The protection capability of the polymer towards O<sub>2</sub> damage was analyzed by means of chronoamperometry, while varying gas mixtures were purged through the electrolyte solution but with a constant supply of H<sub>2</sub> from the backside of the gas diffusion electrode (Figure 3a). When O<sub>2</sub> (5%/95% Ar) enters the electrolyte, the current decreases since some of the electrons liberated from H<sub>2</sub>-oxidation are used by the redox polymer matrix to reduce incoming O<sub>2</sub> molecules.<sup>[23,24]</sup>

After the gas feed was changed back to Ar, the initial currents were restored, indicating efficient protection of the highly sensitive DdHydAB by the polymer matrix even on the porous and rather rough carbon-cloth-based electrode (note that protection is most efficient for homogeneous and smooth polymer/enzyme layers<sup>[24,33]</sup>). This result is in line with our

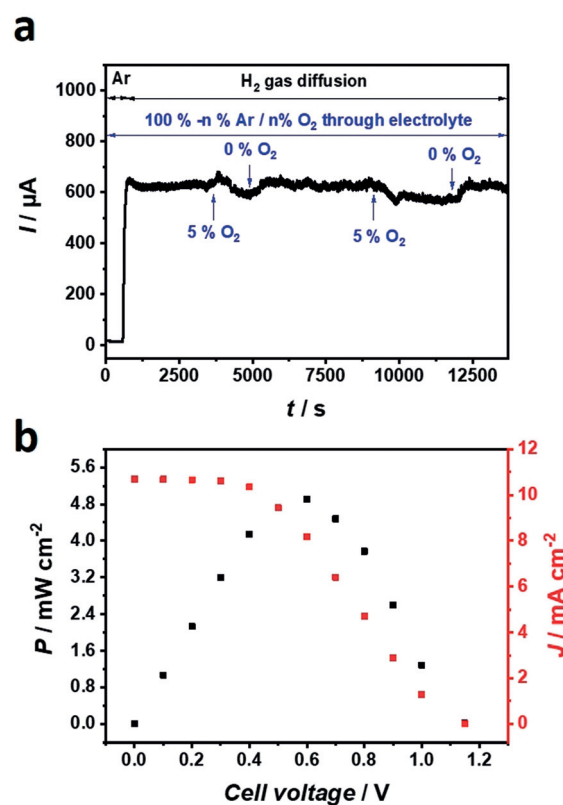


**Figure 3.** Characterization of bioanode stability against O<sub>2</sub> (a) and performance of the H<sub>2</sub>/O<sub>2</sub> biofuel cell equipped with a P(GMA-BA-PEGMA)-vio//P(N<sub>3</sub>MA-BA-GMA)-vio/DdHydAB bioanode (polymer loading:  $1.8 \text{ mg cm}^{-2}$ ) coupled to a Mv-BOx-based biocathode in 0.1 M phosphate buffer, pH 7.4 (b). a) Chronoamperometry at an applied potential of +0.16 V vs. SHE in H<sub>2</sub> gas diffusion mode at changing gas mixtures (Ar (100%) or Ar/O<sub>2</sub> (95%/5%)) purged through the electrolyte; nominal enzyme loading:  $19.9 \text{ nmol cm}^{-2}$ . B) Power curve of the fully assembled membrane-free dual-gas diffusion H<sub>2</sub>/O<sub>2</sub> biofuel cell showing power (left ordinate, black) and current densities (right ordinate, red); nominal enzyme loading:  $39.8 \text{ nmol cm}^{-2}$ .

previous findings concerning gas diffusion electrodes<sup>[20,26]</sup> and for conventional flat glassy carbon electrodes.<sup>[22,23,25]</sup>

To evaluate the performance of the [FeFe]/polymer-based bioanode in a biofuel cell, we combined the H<sub>2</sub>-oxidation electrode with a O<sub>2</sub>-reducing bilirubin oxidase (from *Myrothecium verrucaria*, Mv-BOx) gas diffusion biocathode (see the Supporting information for preparation conditions). The maximum power density of the dual-gas diffusion biofuel cell under anode limiting conditions (Figure S1) was  $5.4 \text{ mW cm}^{-2}$  at 0.7 V, which sets a new benchmark for a biofuel cell equipped with a polymer/hydrogenase-based bioanode (Table S1). The OCV was 1.13 V (recorded after a constant voltage was obtained at open circuit, reached within 3 min) and is only slightly lower than the theoretical value of 1.23 V. Moreover, the value is similar to that of [NiFe]- and [NiFeSe]-based dual-gas diffusion biofuel cells operated in a mediated electron transfer regime<sup>[20]</sup> and in a direct electron transfer regime.<sup>[17,18]</sup> Evidently, the pseudo-capacitive effect of the polymer matrix<sup>[31,32]</sup> compensates for the fact that the redox potential of the viologen is slightly higher than that of the hydrogenase. Cyclic voltammograms recorded with the bio-

anode after biofuel cell tests show identical current values under turnover and non-turnover conditions (Figure S2a). The operational stability of the membrane-free device was tested at a constant load of 0.7 V. The power output decreases after 16 h to 60% of the initial value under continuous operation. This demonstrates the protection capability of the polymer matrix for the sensitive [FeFe] hydrogenase even in a membrane-free device and even outperforms the previously reported polymer/[NiFe] gas diffusion system (50% after 7 h) measured under identical conditions.<sup>[20]</sup> In contrast, when a H<sub>2</sub>-oxidation catalyst with a higher O<sub>2</sub> stability is used as the active material, such as a [NiFeSe] variant,<sup>[34]</sup> the operational stability of the device is drastically enhanced (75% of the initial current remains after 10 h of continuous operation).<sup>[26]</sup> Hence, we can conclude that the overall stability is mainly based on the intrinsic properties of the enzyme.

Cyclic voltammograms recorded with the redox polymer/DdHydAB bioanode and the O<sub>2</sub> reducing biocathode before and after the long-term measurement show that the bioanode (Figure S2a) as well as the biocathode (Figure S1) exhibit a substantial drop in performance. The stability of the anode remains surprisingly high considering the operating conditions (anode limiting conditions in a membrane-free device, operated in a regular fumehood) and the high sensitivity of DdHydAB to immediate O<sub>2</sub> damage.

The maximum current densities ( $J_{\max}$ ) for H<sub>2</sub>-oxidation and the corresponding maximum power density ( $P_{\max}$ ) in the dual-gas diffusion biofuel cell obtained with the DdHydAB [FeFe] hydrogenase are significantly higher than those previously reported for the [NiFe] hydrogenase ( $J_{\max} = 7.9 \text{ mA cm}^{-2}$ ;  $P_{\max} = 3.6 \text{ mW cm}^{-2}$  at 0.7 V),<sup>[20]</sup> the wild-type [NiFeSe] hydrogenase ( $J_{\max} = 5.3 \text{ mA cm}^{-2}$ ),<sup>[20]</sup> and a [NiFeSe] hydrogenase variant<sup>[34]</sup> with enhanced O<sub>2</sub> resistance ( $J_{\max} = 6.3 \text{ mA cm}^{-2}$ ;  $P_{\max} = 4.4 \text{ mW cm}^{-2}$  at 0.7 V)<sup>[26]</sup> (Table S1).

However, when analyzing the solution activities for the individual hydrogenases (Table S1) even higher current densities could be expected for the DdHydAB [FeFe] hydrogenase. Because of the enhanced mass transport under gas diffusion conditions, limitations due to substrate transport can be ruled out. Consequently, electron transport within the redox polymer matrix and/or limitations due to local pH changes because of the massive generation of protons at the electrode–gas–electrolyte interface must be rate limiting. Moreover, the delicate interplay between the individual components (catalyst, redox polymer, and electrode surface) seems to be crucial for the overall activity of the H<sub>2</sub>-oxidation anode. This becomes clear when comparing the enzyme loading for different gas diffusion electrodes (Table S1). In particular, the structurally modified variant of the [NiFeSe] hydrogenase shows outstanding performance even at low catalyst loadings, which was attributed to the enhanced O<sub>2</sub> resistance of this catalyst (all enzymes are in an active state) and a more favored interaction between the polymer matrix/enzyme/electrode interface because of the intrinsic properties of this structurally modified variant, polymer and electrode surface.<sup>[26]</sup> However, the presented results show that even highly sensitive catalysts such as DdHydAB [FeFe] hydrogenase can be successfully incorporated into high-current-density gas diffusion H<sub>2</sub>-oxidation electrodes and can be used

as bioanode in a membrane-free H<sub>2</sub>/O<sub>2</sub> powered biofuel cell with outstanding performance that sets a benchmark with respect to current and power densities under anode-limiting conditions. Moreover, the protection capability of the polymer matrix allows for operation even avoiding complex glovebox systems which is crucial for the transformation of this system to potentially technologically relevant systems.

## Acknowledgements

This work was financially supported by the Deutsche Forschungsgemeinschaft (DFG) within the framework of the Cluster of Excellence RESOLV (EXC-2033; project number 390677874). J.A.B. and W.L. acknowledge funding from the Max Planck Society and J.A.B. acknowledges funding from the Deutsche Forschungsgemeinschaft (DFG) Priority Programme “Iron-Sulfur for Life: Cooperative Function of Iron-Sulfur Centers in Assembly, Biosynthesis, Catalysis and Disease” (SPP 1927) Project BI 2198/1-1. Open access funding enabled and organized by Projekt DEAL.

## Conflict of interest

The authors declare no conflict of interest.

**Keywords:** biofuel cells · gas diffusion electrodes · hydrogenases · molecular hydrogen · redox polymers

- [1] J. R. McKone, S. C. Marinescu, B. S. Brunschwig, J. R. Winkler, H. B. Gray, *Chem. Sci.* **2014**, *5*, 865.
- [2] a) K. P. Sokol, W. E. Robinson, J. Warnan, N. Kornienko, M. M. Nowaczyk, A. Ruff, J. Z. Zhang, E. Reisner, *Nat. Energy* **2018**, *3*, 944; b) T. A. Faunce, W. Lubitz, A. W. Rutherford, D. MacFarlane, G. F. Moore, P. Yang, D. G. Nocera, T. A. Moore, D. H. Gregory, S. Fukuzumi, et al., *Energy Environ. Sci.* **2013**, *6*, 695; c) J. J. Concepcion, R. L. House, J. M. Papanikolas, T. J. Meyer, *Proc. Natl. Acad. Sci. USA* **2012**, *109*, 15560; d) N. S. Lewis, D. G. Nocera, *Proc. Natl. Acad. Sci. USA* **2006**, *103*, 15729; e) A. D. Yoder, *Science* **2013**, *339*, 656; f) M. Grätzel, *Nature* **2001**, *414*, 338; g) A. de Poulpiquet, D. Ranava, K. Monsalve, M.-T. Giudici-Ortoni, E. Lojou, *ChemElectroChem* **2014**, *1*, 1724.
- [3] M. S. Dresselhaus, I. L. Thomas, *Nature* **2001**, *414*, 332.
- [4] F. A. Armstrong, *Science* **2013**, *339*, 658.
- [5] W. Lubitz, H. Ogata, O. Rüdiger, E. Reijerse, *Chem. Rev.* **2014**, *114*, 4081.
- [6] a) A. A. Karyakin, S. V. Morozov, O. G. Voronin, N. A. Zorin, E. E. Karyakina, V. N. Fateyev, S. Cosnier, *Angew. Chem. Int. Ed.* **2007**, *46*, 7244; *Angew. Chem.* **2007**, *119*, 7382; b) A. K. Jones, E. Sillery, S. P. J. Albracht, F. A. Armstrong, *Chem. Commun.* **2002**, 866.
- [7] K. A. Vincent, A. Parkin, F. A. Armstrong, *Chem. Rev.* **2007**, *107*, 4366.
- [8] S. Cosnier, A. J. Gross, A. Le Goff, M. Holzinger, *J. Power Sources* **2016**, *325*, 252.
- [9] I. Mazurenko, X. Wang, A. de Poulpiquet, E. Lojou, *Sustainable Energy Fuels* **2017**, *1*, 1475.
- [10] S. D. Varfolomeev, A. I. Yaropolov, I. V. Berezin, M. R. Tarasevich, V. A. Bogdanovskaya, *Bioelectrochem. Bioenerg.* **1977**, *4*, 314.
- [11] N. Mano, A. de Poulpiquet, *Chem. Rev.* **2018**, *118*, 2392.

- [12] A. Ruff, F. Conzuelo, W. Schuhmann, *Nat. Catal.* **2020**, *3*, 214.
- [13] X. Xiao, H.-q. Xia, R. Wu, L. Bai, L. Yan, E. Magner, S. Cosnier, E. Lojou, Z. Zhu, A. Liu, *Chem. Rev.* **2019**, *119*, 9509.
- [14] P. Rodríguez-Maciá, J. A. Birrell, W. Lubitz, O. Rüdiger, *ChemPlusChem* **2017**, *82*, 540.
- [15] K. So, K. Sakai, K. Kano, *Curr. Opin. Electrochem.* **2017**, *5*, 173.
- [16] A. E. W. Horst, K.-M. Mangold, D. Holtmann, *Biotechnol. Bioeng.* **2016**, *113*, 260.
- [17] S. Gentil, S. M. Che Mansor, H. Jamet, S. Cosnier, C. Cavazza, A. Le Goff, *ACS Catal.* **2018**, *8*, 3957.
- [18] H.-q. Xia, K. So, Y. Kitazumi, O. Shirai, K. Nishikawa, Y. Higuchi, K. Kano, *J. Power Sources* **2016**, *335*, 105.
- [19] a) S. Tsujimura, M. Fujita, H. Tatsumi, K. Kano, T. Ikeda, *Phys. Chem. Chem. Phys.* **2001**, *3*, 1331; b) K. So, Y. Kitazumi, O. Shirai, K. Nishikawa, Y. Higuchi, K. Kano, *J. Mater. Chem. A* **2016**, *4*, 8742.
- [20] J. Szczesny, N. Marković, F. Conzuelo, S. Zacarias, I. A. C. Pereira, W. Lubitz, N. Plumeré, W. Schuhmann, A. Ruff, *Nat. Commun.* **2018**, *9*, 4715.
- [21] J. A. Birrell, K. Wrede, K. Pawlak, P. Rodriguez-Maciá, O. Rüdiger, E. J. Reijerse, W. Lubitz, *Isr. J. Chem.* **2016**, *56*, 852.
- [22] A. A. Oughli, F. Conzuelo, M. Winkler, T. Happe, W. Lubitz, W. Schuhmann, O. Rüdiger, N. Plumeré, *Angew. Chem. Int. Ed.* **2015**, *54*, 12329; *Angew. Chem.* **2015**, *127*, 12506.
- [23] N. Plumeré, O. Rüdiger, A. A. Oughli, R. Williams, J. Vivekananthan, S. Pöller, W. Schuhmann, W. Lubitz, *Nat. Chem.* **2014**, *6*, 822.
- [24] V. Fourmond, S. Stapf, H. Li, D. Buesen, J. Birrell, O. Rüdiger, W. Lubitz, W. Schuhmann, N. Plumeré, C. Léger, *J. Am. Chem. Soc.* **2015**, *137*, 5494.
- [25] A. Ruff, J. Szczesny, S. Zacarias, I. A. C. Pereira, N. Plumeré, W. Schuhmann, *ACS Energy Lett.* **2017**, *2*, 964.
- [26] A. Ruff, J. Szczesny, M. Vega, S. Zacarias, P. M. Matias, S. Gounel, N. Mano, I. A. C. Pereira, W. Schuhmann, *ChemSusChem* **2020** <https://doi.org/10.1002/cssc.202000999>.
- [27] I. Mazurenko, A. de Poulpiquet, E. Lojou, *Curr. Opin. Electrochem.* **2017**, *5*, 74.
- [28] Y. Nicolet, C. Piras, P. Legrand, C. E. Hatchikian, J. C. Fontecilla-Camps, *Structure* **1999**, *7*, 13.
- [29] M. Akter, T. Tokiwa, M. Shoji, K. Nishikawa, Y. Shigeta, T. Sakurai, Y. Higuchi, K. Kataoka, N. Shibata, *Chem. Eur. J.* **2018**, *24*, 18052.
- [30] a) R. A. S. Luz, A. R. Pereira, J. C. P. de Souza, F. C. P. F. Sales, F. N. Crespilho, *ChemElectroChem* **2014**, *1*, 1751; b) M. Rasmussen, S. Abdellaoui, S. D. Minter, *Biosens. Bioelectron.* **2016**, *76*, 91.
- [31] F. Conzuelo, N. Marković, A. Ruff, W. Schuhmann, *Angew. Chem. Int. Ed.* **2018**, *57*, 13681; *Angew. Chem.* **2018**, *130*, 13870.
- [32] S. Alsaoub, F. Conzuelo, S. Gounel, N. Mano, W. Schuhmann, A. Ruff, *ChemElectroChem* **2019**, *6*, 2080.
- [33] a) H. Li, D. Buesen, R. Williams, J. Henig, S. Stapf, K. Mukherjee, E. Freier, W. Lubitz, M. Winkler, T. Happe, et al., *Chem. Sci.* **2018**, *9*, 7596; b) H. Li, D. Buesen, S. Dementin, C. Léger, V. Fourmond, N. Plumeré, *J. Am. Chem. Soc.* **2019**, *141*, 16734.
- [34] S. Zacarias, A. Temporão, M. d. Barrio, V. Fourmond, C. Léger, P. M. Matias, I. A. C. Pereira, *ACS Catal.* **2019**, *9*, 8509.

Manuscript received: May 11, 2020

Accepted manuscript online: May 20, 2020

Version of record online: July 21, 2020